Open Journal of Earthquake Research, 2023, 12, 114-138
https://www.scirp.org/journal/ojer
ISSN Online: 2169-9631
ISSN Print: 2169-9623

The Hidden Earthquake Induced Liquefaction Risks in the Rohingya Refugee Camp Hills & Surrounding Areas of Ukhiya, Cox's Bazar, Bangladesh—A Geotechnical Engineering Approach

Abu Taher Mohammad Shakhawat Hossain[1*], Md. Shakil Mahabub[1], Tanmoy Dutta[1], Mahmuda Khatun[1], Toru Terao[2], Md. Hasan Imam[1], Hossain Md Sayem[1], Md. Emdadul Haque[1], Purba Anindita Khan[1], Sheikh Jafia Jafrin[1]

[1]Geological Engineering, Geohazards & Disaster Sciences Research Group, Department of Geological Sciences, Jahangirnagar University, Dhaka, Bangladesh
[2]Graduate School of Science for Creative Emergence, Kagawa University, Kagawa, Japan
Email: *shakhawathos2004@yahoo.com

How to cite this paper: Hossain, A.T.M.S., Mahabub, Md.S., Dutta, T., Khatun, M., Terao, T., Imam, Md.H., Sayem, H.M., Haque, Md.E., Khan, P.A. and Jafrin, S.J. (2023) The Hidden Earthquake Induced Liquefaction Risks in the Rohingya Refugee Camp Hills & Surrounding Areas of Ukhiya, Cox's Bazar, Bangladesh—A Geotechnical Engineering Approach. *Open Journal of Earthquake Research*, **12**, 114-138.
https://doi.org/10.4236/ojer.2023.123004

Received: May 8, 2023
Accepted: August 13, 2023
Published: August 16, 2023

Abstract

Liquefaction is one of the major catastrophic geohazards which usually occurs in saturated or partially saturated sandy or silty soils during a seismic event. Evaluating the potential liquefaction risks of a seismically prone area can significantly reduce the loss of lives and damage to civil infrastructures. This research is mainly focused on the earthquake-induced liquefaction risk assessment based on Liquefaction Potential Index (LPI) values at different earthquake magnitudes (M = 5.0, 7.0 and 8.0) with a peak ground acceleration (a_{max}) of 0.28 g in the Rohingya Refugee camp and surrounding areas of Ukhiya, Cox's Bazar, Bangladesh. Standard Penetration Test (SPT) results have been evaluated for potential liquefaction assessment. The soils are mainly composed of very loose to loose sands with some silts and clays. Geotechnical properties of these very loose sandy soils are very much consistent with the criteria of liquefiable soil. It is established from the grain size analysis results; the soil of the study area is mainly sand dominated (SP) with some silty clay (SC) which consists of 93.68% to 99.48% sand, 0.06% to 4.71% gravel and 0% to 6.26% silt and clay. Some Clayey Sand (SC) is also present. The silty clay can be characterized as medium (CI) to high plasticity (CH) inorganic clay soil. LPI values have been calculated to identify risk zones and to prepare risk maps of the investigated area. Based on these obtained LPI values, four (4) susceptible liquefaction risk zones are identified as low, medium, high and very high. The established "Risk Maps" can be used for future geological engineering works as well as for sustainable planning, design and construction purposes relating to adaptation and mitigation of seismic hazards in the investigated area.

Keywords

Earthquake, Magnitude, Factor of Safety (Fs), Liquefaction Potential Index (LPI) & Risk

1. Introduction

Liquefaction-induced ground damage is one of the primary causes of infrastructure destruction and this risk requires a critical assessment for sustainable development concerning the safety of engineering structures, design and mitigation measures. As a result, liquefaction hazard maps are becoming increasingly popular and are being incorporated into earthquake risk reduction and mitigation practices globally. Iwasaki *et al.* [1] [2] originally introduced the liquefaction potential index (LPI) for calculating and predicting earthquake-induced liquefaction risks and it has since been widely adopted and developed worldwide [3]-[12]. The LPI values, which simulate the spatial variability of cohesive and non-cohesive alluvial soils with layers of contrasting mixtures, have a clear correlation with the findings of liquefied and non-liquefied soil at particular locations. Bangladesh is surrounded by Himalayan Syntaxis, including the Indo-Burma Folded Belt in the southeast and the Dauki Fault in the northeastern part, which have experienced high-magnitude (M > 7) earthquakes in the past [13]. Two neighboring countries (India and Myanmar) have also faced some great and large-scale earthquakes and the consequences were devastating [14] [15]. Widespread liquefaction events were recorded in the alluvial deposits of Bangladesh after the 1885 Bengal Earthquake, the 1897 Great Indian Earthquake and the 1918 Srimangal Earthquake [16] [17] [18] [19]. Some common consequences of liquefaction were reported as sand boils, settlements and building fragility [20] [21] [22]. According to paleoseismic studies [23] [24] [25], the liquefaction phenomenon in the country's northern and northeastern parts was triggered by a series of seismic events along the Dauki fault. The northeastern and southeastern regions of Bangladesh are the most vulnerable area because of their proximity to the two major sources of earthquakes, *i.e.*, the Dauki Fault [24] and the Indo-Burma Folded Belt [26]. Several researchers predicted that due to ongoing tectonic deformation along the active Dauki fault and Indo-Burman plate boundary faults, medium- to high-magnitude earthquakes might occur in this area [26] [27]. The study area (Ukhiya-Teknaf) is located on this active Indo-Burman plate boundary (**Figure 1**, red-colored box), which is considered for a potential large-scale earthquake [15] [26] [28].

There are a number of active faults (**Figure 1**) in and around Bangladesh as a consequence of the geodynamic development and complex neotectonic evolutions of the Bengal Basin, particularly along its northern and eastern edges. Several of

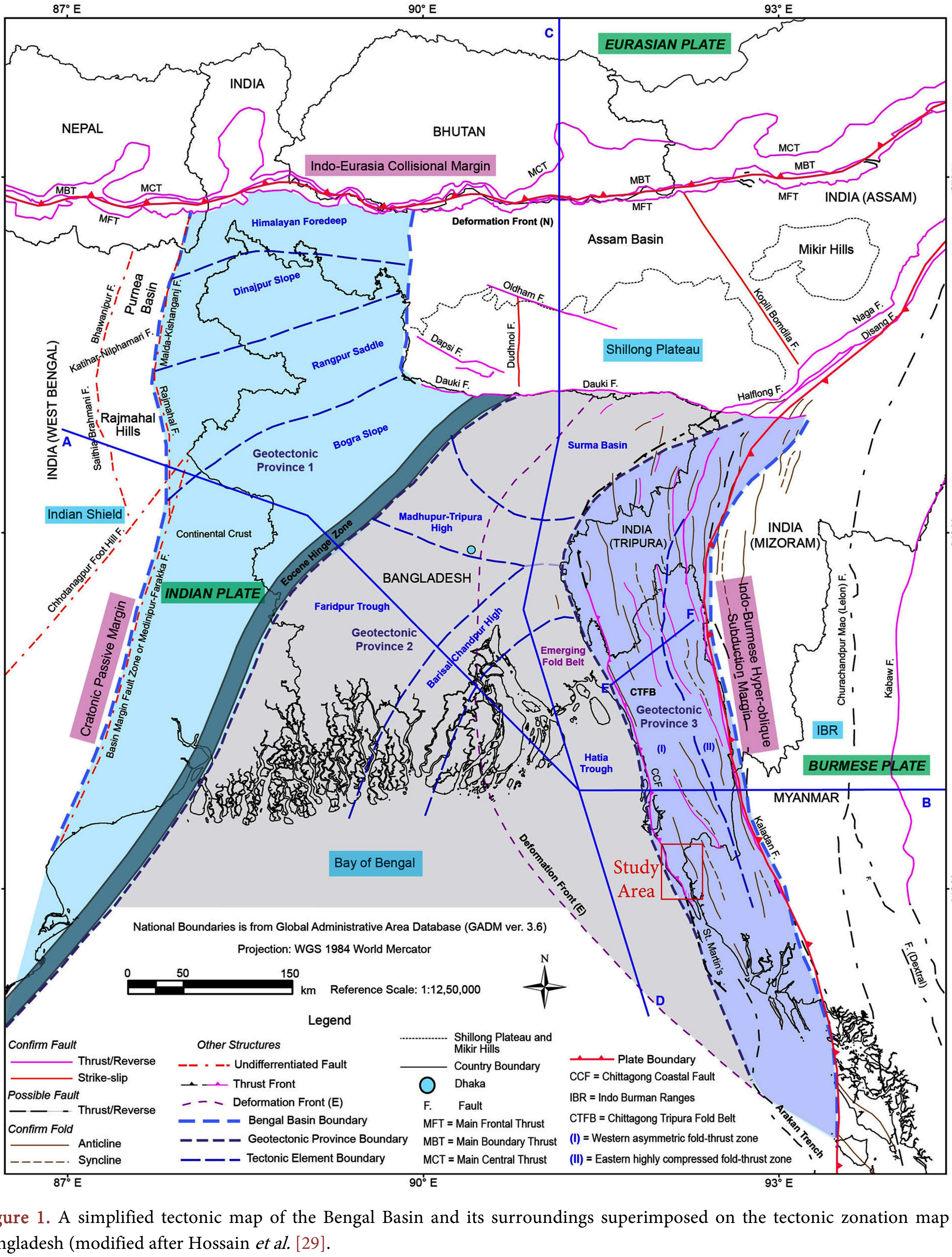

Figure 1. A simplified tectonic map of the Bengal Basin and its surroundings superimposed on the tectonic zonation map of Bangladesh (modified after Hossain *et al.* [29].

these faults are regional and have the potential to produce earthquakes of moderate to large magnitude. The rate of motion and recurrence interval indicates that the probability of earthquakes from the existing active faults is high and an increasing trend of seismic (earthquake) activity has been observed in recent years in and around Bangladesh [18] [29] [30]. The present investigated area is located in seismic zone III (three) with a maximum peak horizontal ground acceleration (PGA) value of a_{max} = 0.28 g according to the Bangladesh National Building Code [31] and shown in **Figure 2(a)**. Historical (light gray, approximate locations) and instrumentally (colored by depth) recorded earthquakes within and around the Chittagong-Myanmar Fold Belt (CMFB) are shown in **Figure 2(b)** based on the prepared map of Bürgi *et al.*, [28] including the depth, hypocenter and magnitudes of earthquake (≥4.0). Latitudinal (ii) and longitudinal (iii) cross sections of instrumental seismicity, where events outlined in gray and black in (i) are plotted in gray and colored by depth, respectively.

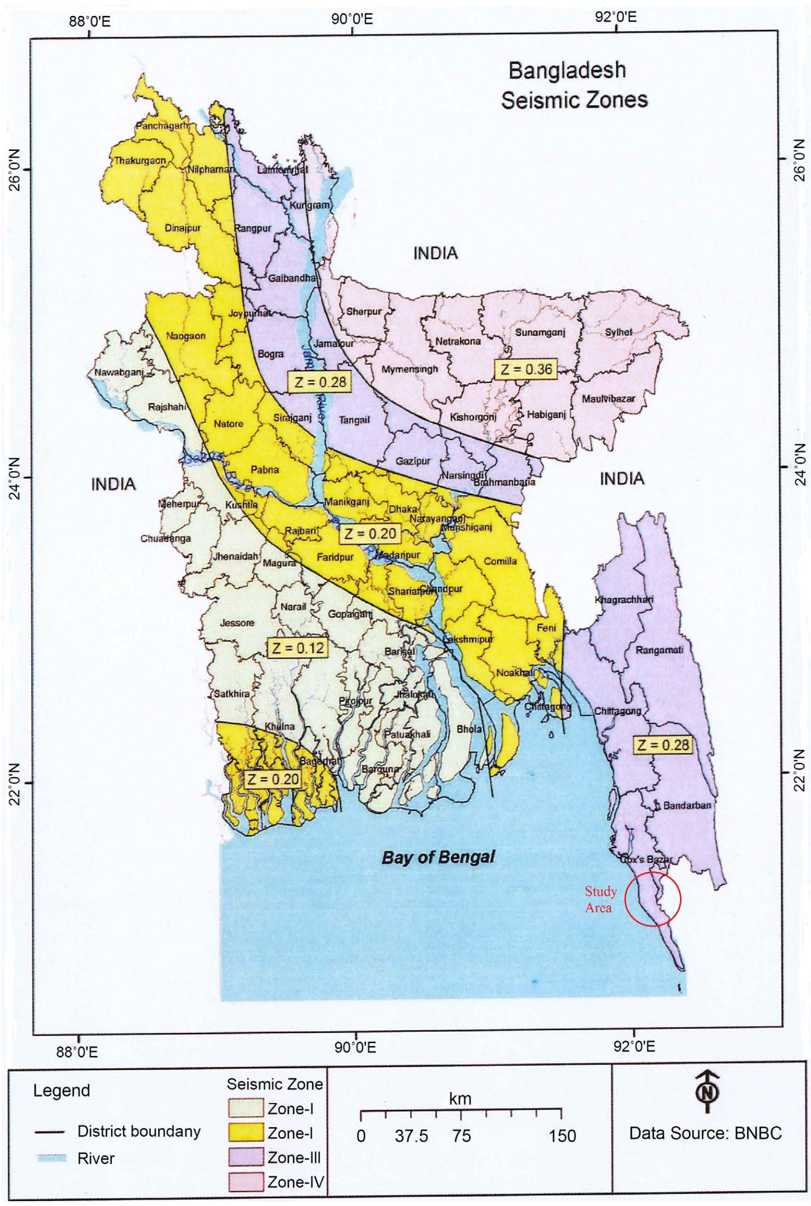

(a)

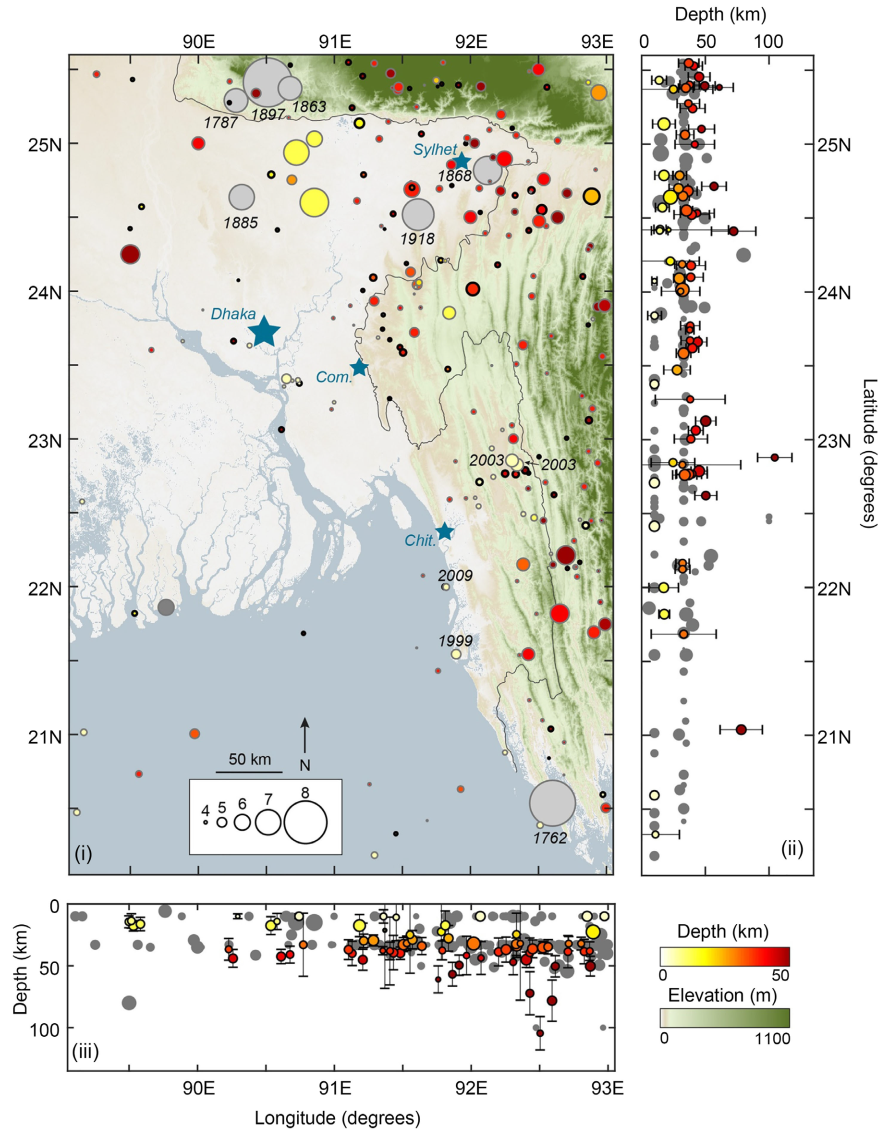

(b)

Figure 2. (a) The seismic zonation map [16] of Bangladesh; (b) Historical (light gray, approximate locations) and instrumentally recorded (colored by depth) earthquakes within and around the Chittagong-Myanmar fold and thrust Belt [28].

Due to mass migration, more than one million Rohingyas were shifted from Myanmar to the Ukhiya-Teknaf hills of Cox's Bazar district, Bangladesh. Hossain *et al.* [32] discussed that Rohingyas live in an anti-humanitarian condition in the Ukhiya hills of Kutubpalong, Balukhali and the Teknaf region [**Figure 3(c)**], where they constructed many temporary shelters by cutting down the hillslopes and trees of the Ukhiya Hills. The typical subsoil profile of Ukhiya and surrounding area consists of yellowish brown very loose to moderately dense medium to fine-grained poorly graded sand (SP) and silty sand (SM). Some earthquake [30] and geohazards incidents have already been reported in recent times [33] in and around the investigated areas.

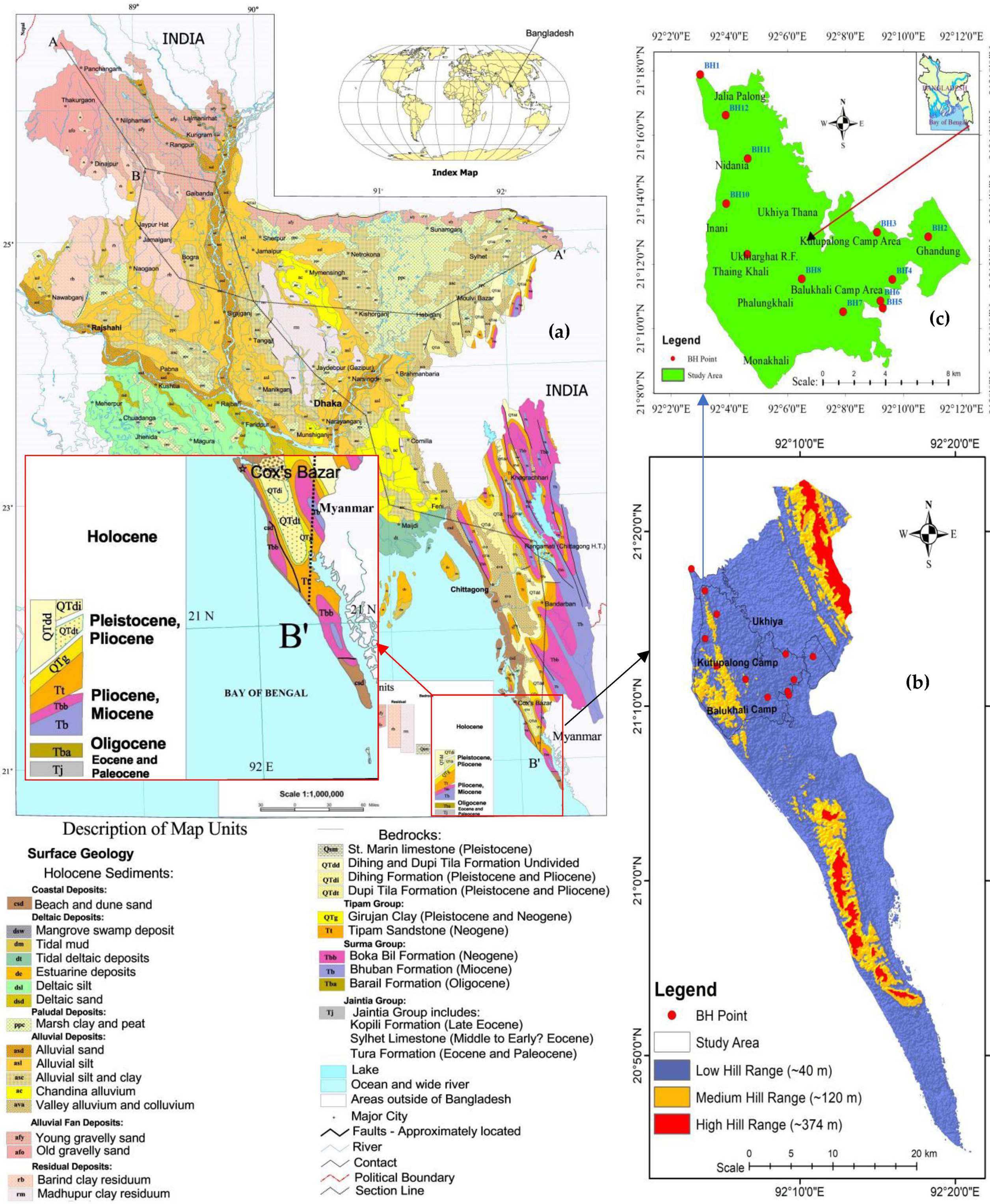

Figure 3. The geological map of Bangladesh (a) modified after Alam *et al.*, [34], geomorphology (b) and location map (c) with boreholes point of the investigated area.

The hidden geohazards, mainly landslides and liquefaction, might occur in the camp and surrounding area, particularly during the rainy season and might create substantial environmental as well as humanitarian disasters. Therefore, people living in these areas are at high risk of landslides and seismic hazards. The general geology, geomorphology and location map with boreholes point of the investigated area are shown in **Figures 3(a)-(c)**.

An earthquake-induced liquefaction might destroy the Ukhiya hills where the Rohingyas constructed temporary shelters and the surrounding area where local communities built up multistoried buildings. Despite this fact, no work has been carried out until 2022 to address the potential risks of seismic liquefaction of the Rohingya refugee camp and surrounding area, Ukhiya, Cox's Bazar, Bangladesh. Mahabub *et al.* [35] carried out a research on the liquefaction hazards of granular soils along the west bank of the Jamuna River, Bangladesh. Hossain *et al.* [32] conducted preliminary research on the risk assessment of the Ukhiya Hills and mentioned the importance of liquefaction risk estimation for a sustainable community living in the camp area. Based on this preliminary work, Dutta [36] conducted a detailed research investigation funded by ANSO (the Alliance of International Science Organizations) China to identify earthquake-induced liquefaction risks in the Ukhiya Hills at different earthquake magnitudes. They conducted a thorough investigation to identify risks and emphasized the importance of developing risk maps based on LPI values for urban planning, design and construction of engineering infrastructures for sustainable community living for the Rohingyas, where Rohingyas constructed temporary shelters. Moreover, Hossain *et al.* [32] and Imam *et al.* [37] reported on the hidden geohazards and site conditions of the Rohingya refugee camp area.

This research mainly focuses on the liquefaction potentiality and risk assessment of the Rohingya refugee camps and surrounding areas of Cox's Bazar based on LPI values at three earthquake mag-nitudes (5.0, 7.0 and 8.0). These earthquake magnitudes were considered for the liquefaction potentiality analyses from the 165 years of historical earthquake records [31] at peak ground acceleration values of 0.28 g for seismic zone III. Based on the framework, the factor of safety, Fs = (CSR/CRR), was determined at the average depths of each soil layer to address liquefaction potential. The liquefaction potential severity at the targeted depth was then evaluated by the liquefaction potential index (LPI) proposed by Iwasaki *et al.* [1] [2] and Luna & Frost [10]. Moreover, the findings are represented on maps to demonstrate the applicability and sensitivity of the proposed framework for liquefaction potential risks.

2. Materials and Methods

A detailed geotechnical site investigation was carried out in the investigated area in accordance with British Standards (BS) 5930 [38] to characterize the soils and evaluate the liquefaction potential. Twelve boreholes were drilled in the project area (Ukhiya) to collect disturbed and undisturbed samples. Liquefaction hazard based on factor of safety and settlements were calculated by LiquefyPro Ciivl-Tech (2015) software [39]. Output parameters were determined by giving SPT value, depth, ground water level, fines content, unit weight, lithlogy, earthquake magnitude & peak ground acceleration (PGA) value parameters. SPT (N) numbers were recorded to interpret the ground condition. The light cable percussion drilling method was used for collecting samples and the wash boring technique was used as a means of advancing the borehole to enable the taking of tube samples. Geotechnical parameters were determined from laboratory experiments according to BS 1377 [40] and the American Society for Testing and Materials (ASTM) standards [41].

Assessing liquefaction potential is a critical task in geotechnical earthquake engineering. There was no alternative method to evaluate liquefaction potential except the factor of safety (Fs) until 1982. However, it is difficult to evaluate the liquefaction susceptibility and its risk potential at any site solely based on the factor of safety (Fs). As a result, factor of safety (Fs) and the liquefaction potential index (LPI) were applied simultaneously for assessing potential liquefaction risk in this research. The LPI has been used as a popular tool due to the inclusion of thickness, depth and safety factors for a particular soil layer to evaluate the liquefaction and potential foundation damage. Therefore, the proposed framework for liquefaction potentiality and risk assessment is shown in the flowchart (**Figure 4**).

This research utilized an empirical criterion based on SPT–N values to calculate the factor of safety (Fs). Seed and Idriss [42] proposed this simplified procedure based on SPT-N values to evaluate the liquefaction resistance of soils and this method has been modified and improved over the years [42]-[49]. Later, Youd *et al.* [50] proposed the following form:

Compute the cyclic stress ratio (CSR), which is related to the peak acceleration ($a_{\max}$) at the ground surface during the design earthquake formulated by Seed and Idriss [42]:

$$\text{CSR} = \frac{\tau_{av}}{\sigma_0'} = 0.65\left(\frac{a_{\max}}{g}\right)\left(\frac{\sigma_0}{\sigma_0'}\right)r_d \tag{1}$$

where,

τ_{av} = average cyclic shear stress induced by design ground motion;

σ_0' = initial static effective overburden stress on sand layer under consideration;

σ_0 = initial total overburden stress on sand layer under consideration;

$a_{\max}$ = peak horizontal acceleration in g's;

r_d = a stress reduction factor varies from a value of 1.0 at ground surface to 0.5 at a depth of about 30 m.

The following equation computes the cyclic resistance ratio (CRR) according to Youd *et al.* [50].

$$\text{CRR} = \text{CRR}_{7.5} \cdot \text{MSF} \tag{2}$$

$\text{CRR}_{7.5}$ is the cyclic resistance ratio for magnitude 7.5 earthquakes and can be calculated by:

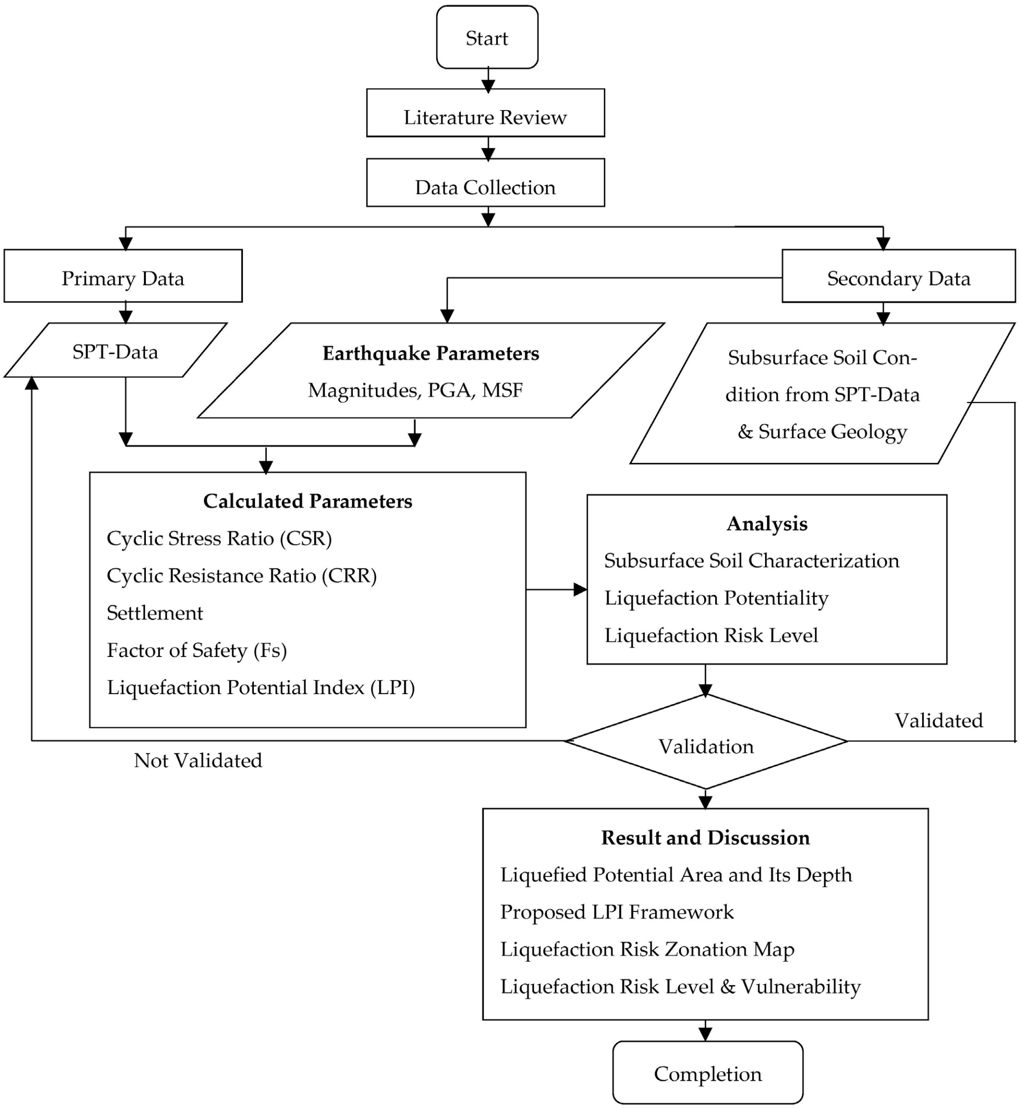

Figure 4. The proposed framework for evaluating liquefaction risks in the investigated area.

$$\mathrm{CRR}_{M=7.5} = \frac{1}{34-(N_1)_{60}} + \frac{(N_1)_{60}}{135} + \frac{50}{\left[10\cdot(N_1)_{60}+45\right]^2} - \frac{1}{200} \quad (3)$$

MSF is the magnitude-scaling factor used for magnitudes smaller or larger than 7.5. The MSF is calculated by Seed and Idriss [44]:

$$\mathrm{MSF} = \frac{10^{2.24}}{M_w^{2.56}} \quad (4)$$

Cyclic resistance ratio (CRR) expresses the capacity of soil to resist liquefaction. CRR is determined from the curves, which show the correlation between corrected SPT blow-count [$N_{1(60)}$] and the Cyclic Stress Ratio (CSR). It has been suggested that the corrections (SPT value) should be applied according to the following formula [51]:

$$N_{1(60)} = N_m C_N C_e C_b C_r C_s \quad (5)$$

where,

N_m = SPT raw data, measured standard penetration resistance from field;

C_N = depth correction factor;

C_e = hammer energy ratio (ER) correction factor;

C_b = borehole diameter correction factor;

C_r = rod length correction factor;

C_s = correction factor for samplers with or without liners.

The following equation presents the results of the liquefaction assessment with a factor of safety (Fs) values against liquefaction.

$$\text{Fs} = \frac{\text{CRR}}{\text{CSR}} = \frac{\text{CRR}_{7.5}}{\text{CSR}} \times \text{MSF} \tag{6}$$

The determined factor of safety (Fs) did not include two other essential criteria. However, the thickness and depth of the liquefiable soil layer and the factor of safety are crucial inputs for damage potential based on liquefaction and that was proposed and assessed by Iwasaki *et al.* [1] [2]. According to Iwasaki *et al.* [1] [2], the potential risks are determined based on the LPI in the following ways:

$$\text{LPI} = \int_0^{20} F(z)w(z)\text{d}z \tag{7}$$

$F(z) = 1 - \text{Fs}$ for $\text{Fs} < 1.0$;

$F(z) = 0$ for $\text{Fs} \geq 1.0$;

$w(z) = 10 - 0.5z$ for $z < 20$ m [where, z = depth in meter];

$w(z) = 0$ for $z > 20$ m.

Where z is the depth of the midpoint of the soil layer (0.0 to 20.0 m) and dz is the differential increment of depth. The weighting factor, $w(z)$ and the severity factor, $F(z)$, are calculated according to the expressions mentioned above.

For the soil profiles with a depth of less than 20.0 m, LPI is calculated using the following expression [2] [10]:

$$\text{LPI} = \sum_{i=1}^{n} w_i F_i H_i \tag{8}$$

And, $F_i = 1 - \text{Fs}_i$ for $\text{Fs}_i < 1.0$;

$F_i = 0$ for $\text{Fs}_i \geq 1.0$.

Where H_i is the thickness of discretized soil layers; n is the number of layers; F_i is liquefaction severity for i-th layer; Fs is the factor of safety for i-th layer; w_i is the weighting factor (=10 - 0.5z) and z is the depth of i-th layer (m).

Therefore, it can be summarized that, within this paper's scope, the soil's liquefaction susceptibility has been evaluated based on a simplified approach, modified by Youd *et al.* [50] and settlement of soils has been calculated by the Tokimatsu and Seed [48] method. Finally, the potential risks were determined based on Liquefaction Potential Index (LPI), which included the factor of safety (Fs) and was calculated from the software's [52] output based on SPT value, fine content, unit weight, lithology, earthquake magnitude (M), peak ground acceleration (PGA), depth and groundwater level input data. The determined Fs (CRR/CSR) values were then used to calculate the LPI values. Whereas, LPI assumes that the severity of liquefaction is proportional to (1) the thickness of the liquefied layer, (2) the proximity of the liquefied layer from the ground surface and (3) the amount by which the factor of safety (Fs) is less than 1.0 for liquefiable soil layers.

3. Results and Discussion

Potential risk assessments for earthquake-induced liquefaction are important for reducing threats, implementing mitigation measures and promoting long-term development in an area. Total risk is associated with the ground of the investigated area and its soil types, grain size, density, groundwater level, settlement, age, peak ground acceleration values and possible seismic events. This research assesses potential risk based on the factual data, field and laboratory test results of collected soil samples from the Rohingya refugee camp area. The basic geotechnical properties of some soils are listed in **Table 1**.

A total of 23 samples were collected from different sites at particular depths and analyzed by both dry and wet sieve testing methods. The obtained data from the grain size test result shows 95.23% Sand, 2.94% Gravel and 1.83% Silt & Clay. The grading properties of soil, such as uniformity coefficient (Cu) and coefficient of curvature (Cc) vary from 1.56 - 5.06 and 0.96 - 1.32 and these properties suggest that these soils are loose to very loose, poor to well-graded sandy soil (SP-SW) with fine content of less than 5% and consistent with USCS classification [53] and have a substantial influence on liquefaction. From the grain size distribution curves (**Figure 5**), it is observed that the soils are mainly uniformly graded and sand samples fall within the range of 0.05 to 2.0 mm, which indicates that these soils are susceptible to liquefy and the results are completely consistent with Tsuchida [54] and Iwasaki [55].

Table 1. Basic Geotechnical properties of the Rohingya refugee camp area.

Camp Name	Depth (m)	Sample No.	Grain Size (%)			Grading Properties		Moisture Content	Specific Gravity	Cohesion (c)	Angle of Internal Friction
			Gravel	Sand	Silt + Clay	Cu	Cc	(%)	-	kPa	Degree
Kutupalong Rohinghya Camp	0.60 - 1.06	D-1	0.56	98.41	1.03	2.05	1.10	25.45	2.59	-	-
	2.13 - 2.59	D-2	10.03	88.95	1.02	5.06	1.32	29.39	2.56	7.04	26.38
	3.65 - 4.11	D-3	17.11	82.09	0.80	4.30	1.14	18.53	2.55	-	-
	5.18 - 5.63	D-4	4.69	94.70	0.61	2.92	1.26	18.87	2.60	9.92	27.79
	6.24 - 6.71	D-5	1.20	97.74	1.06	1.93	1.07	19.26	2.53	13.95	26.76
Bhalukhali Rohinghya Camp	0.60 - 1.06	D-1	0.48	98.88	0.64	2.41	1.09	13.96	2.59	-	-
	2.13 - 2.59	D-2	0.18	99.48	0.34	1.92	1.11	13.19	2.56	4.48	34.29
	3.65 - 4.11	D-3	1.63	97.37	1.00	2.42	1.21	13.04	2.55	17.40	16.75
	5.18 - 5.63	D-4	0.38	99.04	0.58	1.78	1.02	24.64	2.60	-	-
	6.70 - 7.16	D-5	0.77	98.65	0.58	2.64	0.97	20.07	2.53	13.43	23.46
	8.22 - 8.68	D-6	0.53	99.35	0.12	1.56	0.96	25.02	2.55	-	-

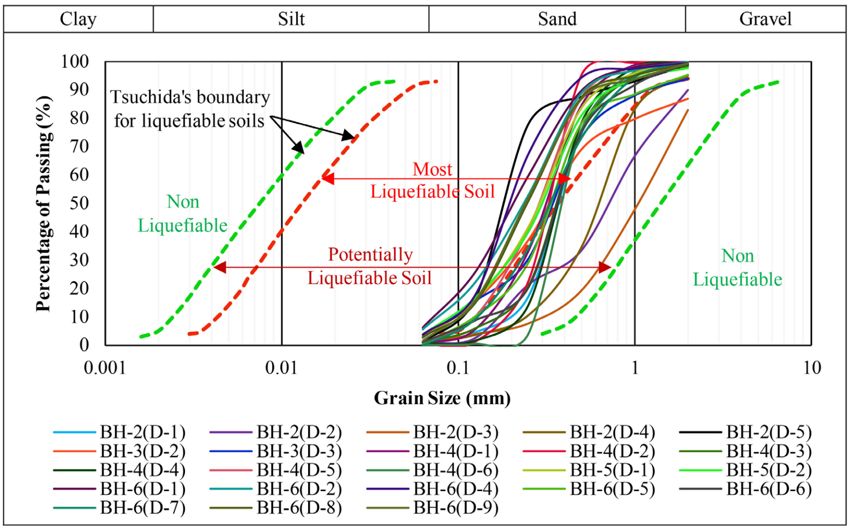

Figure 5. Particle size distribution of the study area.

The natural moisture content values of selected disturbed samples from the camp area range from 13.04% to 29.39% and these obtained moisture contents show consistency with the moisture content values quoted by Bowles [56]. The specific gravity values of the investigated area lie between 2.52 and 2.60, which indicates that this soil is predominately cohesionless granular soil and the obtained specific gravity values are closer to the recommended values of Grim [57] and Bowles [56]. From the direct shear testing, a cohesion (c) value ranging from 4.48 to 17.40 and an angle of internal friction (φ) ranging from 16.75˚ to 34.23˚ are measured and these results show initially a rapid increase in shear strength with increasing shear displacement, while after reaching a shear displacement of 200 mm, the shear strength increases slowly and reaches a peak value of 40 kPa before it starts to decline. The shear strength parameter indicates that these soils are granular very loose to loose sandy soils and consistent with (c) and (φ) values suggested by Bowles [58]. These recently deposited poorly compacted Holocene to Pleistocene soil, such as channels deposit and Dupi Tila formation, are susceptible to liquefaction because of sandy soil's low shear strength and dilatancy nature which triggered liquefaction during a seismic event due to the increase in pore water pressure.

Considering the high importance of constructing temporary shelters for the community living in the Ukhiya hills for millions of refugees, including local people in the Ukhiya-Teknaf area, this study attempts to evaluate the factors of safety (Fs) against liquefaction and corresponding liquefaction potential indices (LPI) for the worst seismic scenario for the refugee camps and surrounding area using an SPT-based semiempirical procedure. The factor of safety (Fs) values for the study area are shown in **Figure 6** at variable depths for magnitudes 5.0, 7.0 and 8.0 in both dry and wet seasons. The graphical distribution (**Figure 6**) shows the comparative relations of the factor of safety (Fs) values against depths in the dry and wet seasons for three different earthquake magnitudes; if the Fs values are less than 1.0 that represents a liquefiable soil layer and is marked as a red point. In contrast, if the factor of safety (Fs) is greater than 1.0, the soil is non-liquefiable and represents itself as a green marker. It is evident from the charts that the liquefiable soil is concentrated at depths ranging from 0.5 m to 10.0 m for lower magnitudes (5.0), but it extends below these depths with up to 15.0 m for higher earthquake magnitudes (7.0 and 8.0). Moreover, a distinct variation was observed in the case of dry and wet seasons for each particular magnitude. Lower factor of safety (Fs) values was observed at higher earthquake magnitudes.

According to Figure 7, the CRR and CSR against depth curves have been evaluated in the dry and rainy seasons. It has been noted that CRR values are highly variable throughout the dry and wet seasons, varying from 0.05 to 1.25 for the dry season and 0.05 to 1.0 for the rainy season. At low earthquake magnitudes (M = 5.0), CRR values are high and at higher magnitudes (M = 7.0 & 8.0), the obtained values are low (<0.5). On the other hand, a close consistency was observed between the CSR and depth curves for the dry and wet seasons. The obtained CSR values range from 0.18 to 0.40. The variation in CSR values is not significant at greater depths but is prominent at shallow depths (Figure 7).

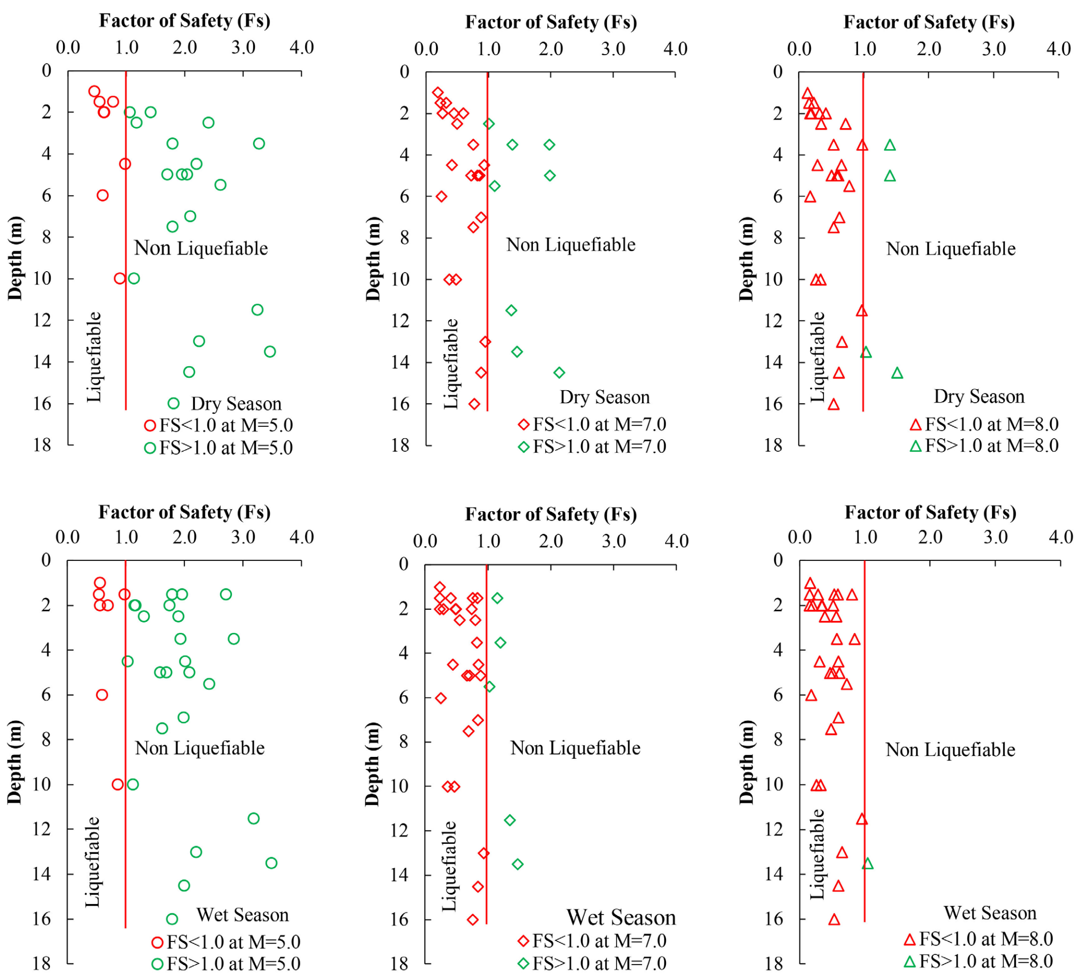

Figure 6. The factor of safety (Fs) against liquefaction at particular depths for earthquake magnitude (M = 5.0, 7.0 & 8.0) with a peak ground acceleration of 0.28 g.

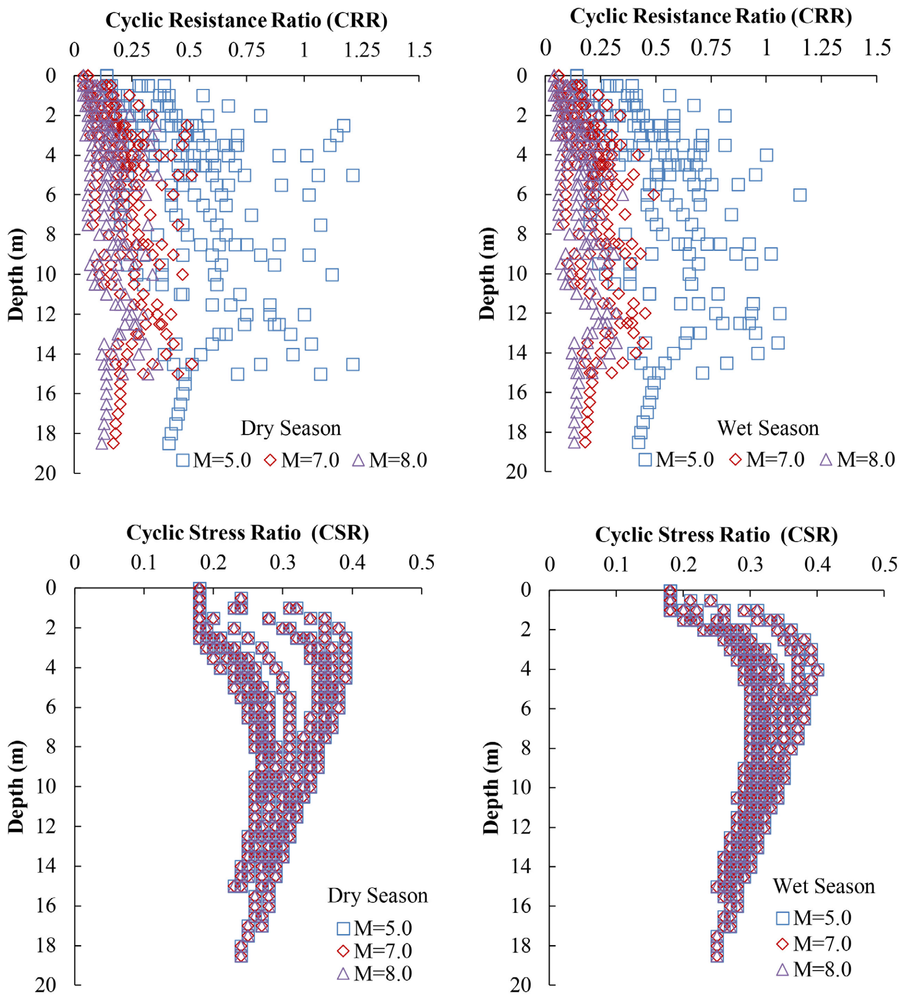

Figure 7. Variation of CRR and CSR with depths at different earthquake magnitudes during liquefaction assessment.

Settlement of soil is a common phenomenon that occurs during liquefaction in loose sandy soils and affects ground structures. Settlement of the dry and wet (saturated) soil was calculated based on the Tokimatsu and Seed [48] method for all three magnitudes. However, it has shown a slight variation because of the difference between the dry and wet seasons, but it remains steady for three magnitudes (**Figure 8**). The maximum and minimum settlements observed at this site are around 30 cm and 25 cm for low and high earthquake magnitudes, respectively. The settlement amount decreases with increasing depth. The thickness of the potential liquefiable soil layer is consistent with soil settlement. A resemblance is observed between these three magnitudes in terms of potential liquefaction depths based on the settlement amount (**Figure 8**).

The seismic soil liquefaction potential index (LPI) is determined for 12 specific sites across the Rohingya Refugee camp and surrounding area. The contour maps based on LPI values are generated for the camp to show the spatial distribution of liquefaction potential and these maps indicate the geographic variability of liquefaction effects and different possible surface manifestations of liquefaction. The spatial distribution of soil liquefaction potential for earthquakes with a 2% probability of exceedance is quantitatively presented in the form of contour maps showing the liquefaction potential index (LPI). The risk maps of LPI are prepared for the investigated area to predict the occurrence of potential damage by liquefaction for the earthquake magnitudes M = 5.0, 7.0 and 8.0 (in Richter scale) at maximum peak ground acceleration (0.28g) corresponding to the seismic event for the 2475-year return period. LPI versus depth curves at different earthquake magnitudes (M = 5.0, 7.0 and 8.0) are shown in **Figure 9**. From the illustration, a distinct variation in LPI values is observed between low and high earthquake magnitudes in terms of LPI values and depths in both seasons. LPI is approximately 15.0 (0.0 - 15) for low earthquake magnitude (5.0) but greater than 15.0 (0.0 - 30) for high magnitudes (7.0 and 8.0) at shallower depths (<10.0 m). However, LPI values are extended up to 15.0 m for larger magnitudes which are not observed at lower depths.

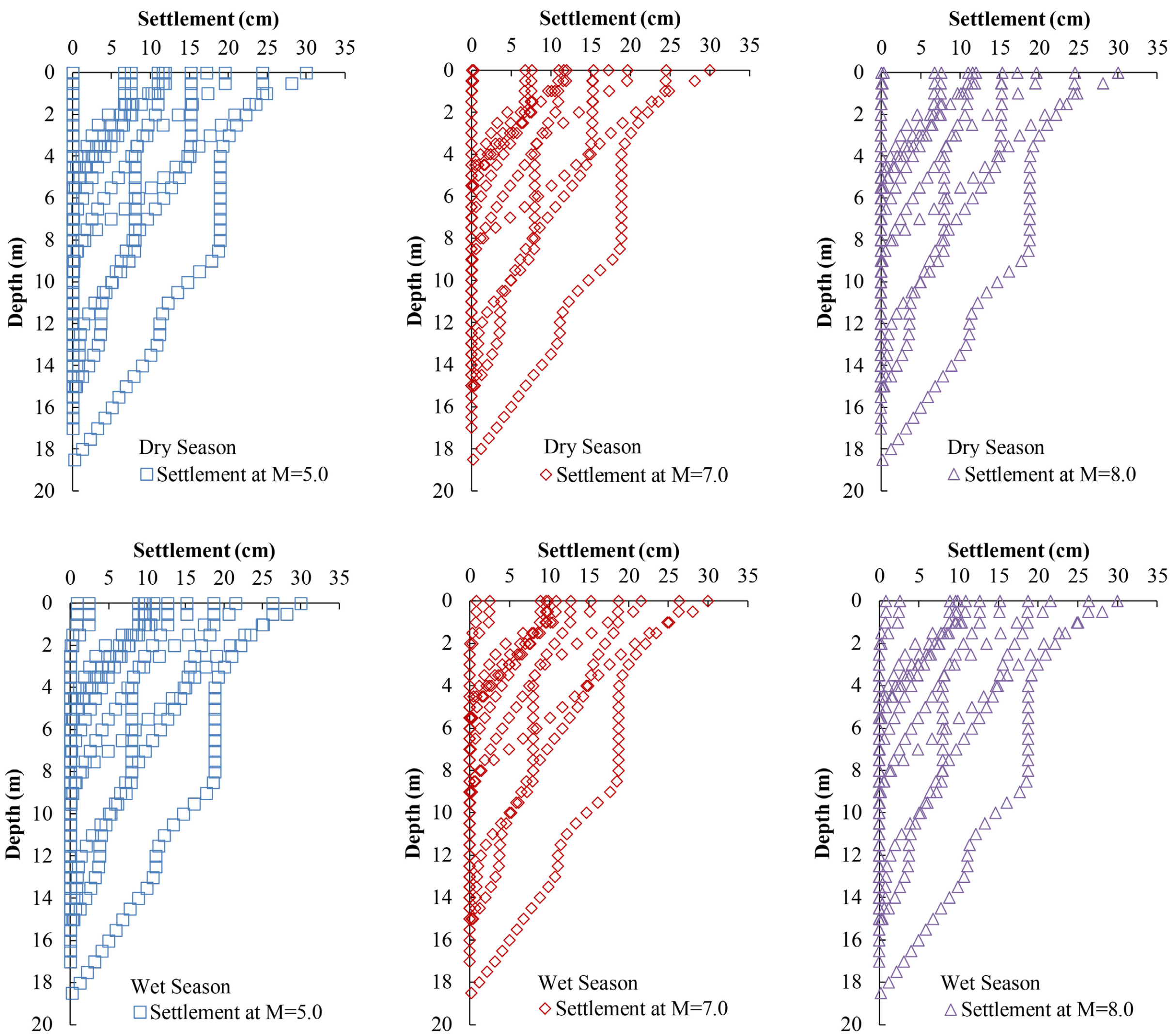

Figure 8. Settlement versus depth curves for dry and wet conditions at different earthquake magnitudes (M = 5.0, 7.0 & 8.0).

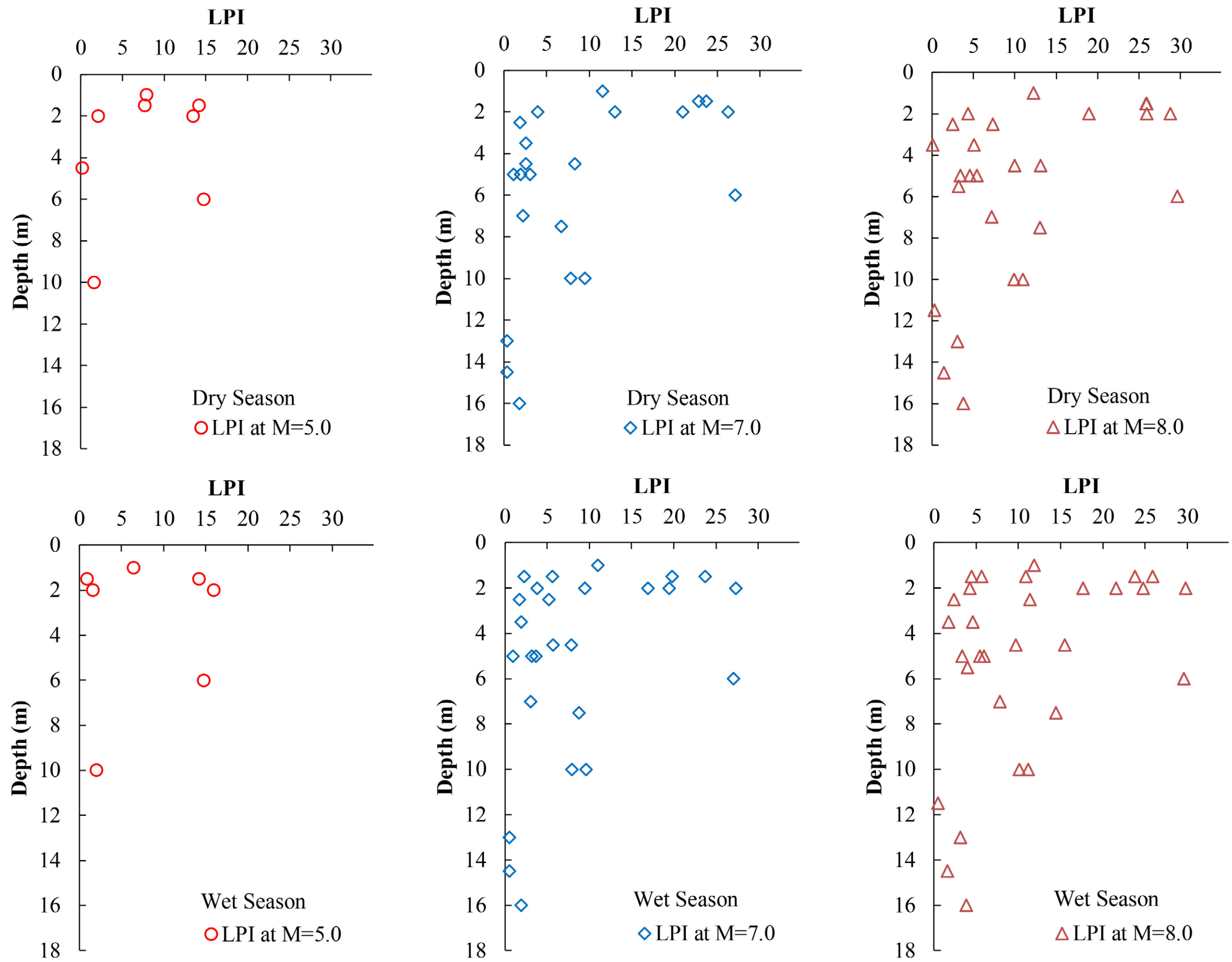

Figure 9. Liquefaction potential index (LPI) against depths for earthquake magnitude, M = 5.0, 7.0 & 8.0.

The potential risk for liquefaction is evaluated and classified based on LPI values suggested by several researchers [2] [3] [10] [12]. This research proposes a new classification by modifying the existing classifications for wide ranges of LPI values, as shown in **Table 2**. Liquefaction risk maps are produced using determined LPI values for different earthquake magnitudes (**Figure 10**, **Figure 11**) are listed in **Table 3**. These risk maps show the liquefaction vulnerability at Ukhyia and some parts of Teknaf, including the Rohingya refugee camps, particularly Balukhali and Kutubpalong areas. Liquefaction susceptibility values for some sites are very high (LPI > 25) and are very unlikely or low at other sites (LPI < 5). Some of the sites in the camp, namely Kutubpalong, Balukhali and Nidania region, are highly vulnerable to severe liquefaction for high earthquake magnitudes (M = 7.0 and 8.0) and the LPI values are higher than 25. However, for the same area, the potential risk is medium (LPI ≤ 15) and low (LPI < 5) for low magnitudes (M = 5.0).

The calculated LPI values are listed in **Table 3** and compared with the boreholes at different earthquake magnitudes (5.0, 7.0 and 8.0) for dry and wet seasons. The comparison between the dry and wet seasons LPI results established that the potential risk of soil liquefaction is increased with an increase in the earthquake magnitude and groundwater level. Based on estimated LPI values at different earthquake magnitudes, four (4) susceptible liquefaction potential risk zones are identified in the Rohingya refugee camp and surrounding area, as shown in the prepared risk maps (Figure 10, Figure 11). These are classified as low (0 < LPI ≤ 5), medium (5 < LPI ≤ 15), high (16 < LPI ≤ 25) and very high (26 < LPI ≤ 56) risk zones. According to this classification, the variation in risk categories for many locations changes from none or low to medium; medium to high; and high to very high due to the seasonal variations (dry to wet seasons), even though other parameters remain constant.

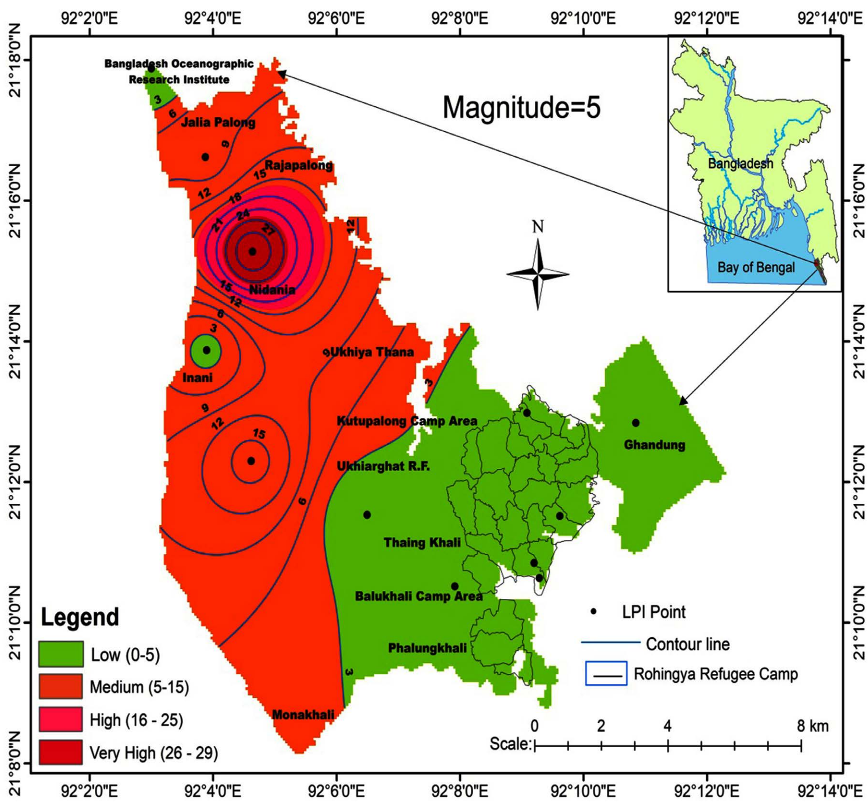

Figure 10. Risk map based on liquefaction potential index (LPI) at low earthquake magnitude (M = 5.0).

Table 2. LPI-based risk classification of the Rohingya refugee camp area and comparison with other authors.

LPI	Iwasaki *et al.* [2]	Luna and Frost [10]	Toprak and Holzer [12]	Chung and Rogers [3]	This Research
0	Not Likely	Little to None	None	None	None
0 < LPI ≤ 5	Not Likely	Little to None	Low	None	Low (0 < LPI ≤ 5)
5 < LPI ≤ 15	-	Moderate	Medium	Moderate	Medium (5 < LPI ≤ 15)
15 < LPI ≤ 100	Severe	Major	High	Severe	High (16 < LPI ≤ 25) Very High (26 < LPI ≤ 56)

Table 3. LPI and degree of risks at different earthquake magnitudes and locations during dry and wet seasons.

Boreholes No.	Earthquake Magnitude (M)	Dry Seasons		Wet Seasons	
		Liquefaction Potential Index (LPI)	Sensitivity & Risks	Liquefaction Potential Index (LPI)	Sensitivity & Risks
BH-01	5.0	0.00	None	0.00	None
	7.0	0.00	None	5.75	Medium
	8.0	0.00	None	11.02	Medium
BH-02	5.0	0.00	None	0.00	None
	7.0	0.00	None	0.00	None
	8.0	0.00	None	4.55	Low
BH-03	5.0	0.00	None	0.00	None
	7.0	9.43	Medium	15.26	High
	8.0	20.14	High	30.15	Very High
BH-04	5.0	0.00	None	0.00	None
	7.0	2.73	Low	5.85	Medium
	8.0	13.25	Medium	15.59	High
BH-05	5.0	0.00	None	0.00	None
	7.0	5.57	Medium	12.27	Medium
	8.0	20.39	High	25.45	Very High
BH-06	5.0	0.00	None	0.00	None
	7.0	0.00	None	9.62	Medium
	8.0	3.35	Low	21.87	High
BH-07	5.0	8.05	Medium	1.01	Low
	7.0	31.37	Very High	27.91	Very High
	8.0	36.12	Very High	33.81	Very High
BH-08	5.0	0.00	None	0.00	None
	7.0	22.37	High	20.65	High
	8.0	29.64	Very High	28.40	Very High
BH-09	5.0	13.54	Medium	16.04	High
	7.0	34.30	Very High	35.53	Very High
	8.0	38.93	Very High	40.16	Very High
BH-10	5.0	1.68	Low	2.14	Low
	7.0	25.19	High	29.56	Very High
	8.0	37.28	Very High	40.16	Very High
BH-11	5.0	29.12	Very High	29.12	Very High
	7.0	51.06	Very High	51.06	Very High
	8.0	55.76	Very High	55.76	Very High
BH-12	5.0	10.08	Medium	8.20	Medium
	7.0	20.48	High	18.86	High
	8.0	24.74	High	23.52	High

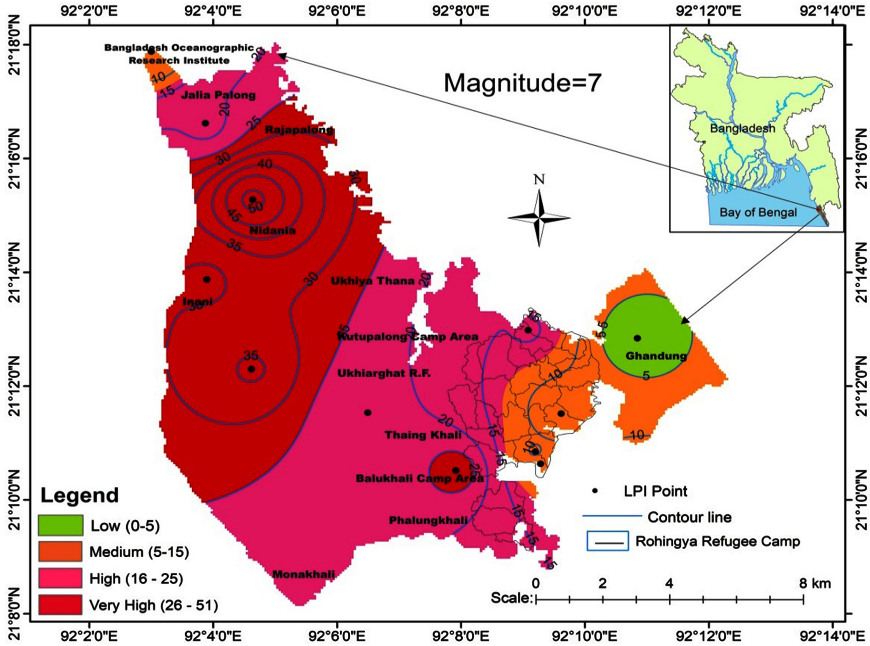

(a) At earthquake magnitude (M = 7.0)

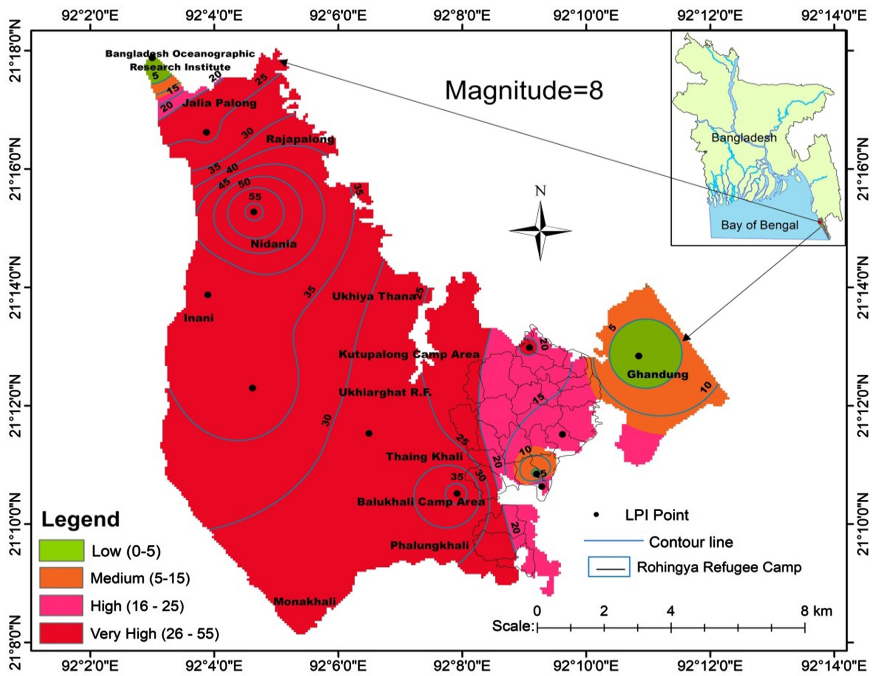

(b) At earthquake magnitude (M = 8.0)

Figure 11. Risk maps [(a), (b)] based on liquefaction potential index (LPI) at high earthquake magnitudes (M = 7.0 and 8.0).

From the overall observations, it is established that the Rohingya refugee camp area has a medium to very high potential for liquefaction based on sensitivity and risk analyses. The areas consist of Dupitila and Recent sediment (channel deposits) and have a considerable thickness of loose soil deposits with shallow groundwater levels. These soils are more susceptible to liquefaction during the rainy seasons because of the increased pore water pressure and higher water table. This study reveals that the higher susceptibility (**Figure 10**) of liquefaction at some places (Nidania, Rajpalong) can be attributed to the higher thickness of soft, loose soil deposits and higher groundwater tables at shallow depths for low earthquake magnitudes (M = 5.0). It can also be observed from the LPI contour maps (**Figure 10**, **Figure 11**) that a high degree of liquefaction damage is likely to occur at several sites, such as Kutubpalong and Balukhali in the Rohingya refugee camp area, during a severe (high) seismic event of magnitude 7.0 or greater (**Figure 11**).

Moreover, there is no proper balance between social, economic and environmental aspects in the Rohingya refugee camp area and sustainability is very much neglected. Sustainable development is a constitutional obligation in Bangladesh. It is not reflected in the refugee camp area as per UN sustainable development goals [59]. Lack of resilient infrastructures, a lack of a peaceful society, healthy lives, scarcity of drinking water and sanitation and loss of biodiversity, wetlands and forests in the camp area threaten the overall sustainability of the camp hills [60]. By destroying the green, wooded eco-forest of Ukhiya, Rohingyas constructed temporary shelters on the loose, unconsolidated sandy soils, which are at high risk of seismic events. Furthermore, there is no sustainable management of forests in the camp area.

4. Conclusion & Recommendations

Based on the overall observations, it is established that the Rohingya refugee camp hill soils are medium to highly susceptible to liquefaction risk at earthquake magnitudes 5.0 or above, up to a depth of (±) 10.0 m but at lower magnitudes (M < 5.0), these soils are non-liquefiable (Fs > 1.0). Moreover, this depth is extended to around 15.0 m for the higher magnitudes (M = 7.0 and 8.0) with a factor of safety (Fs) value < 1.0. The determined grain size results, uniformity of soil, sand content, pore water pressure change, geological material characteristics and other geotechnical properties are very much consistent with the criteria of liquefiable soils. Based on the determined LPI values, four (4) susceptible liquefaction potential risk zones are identified and these are summarized as low (LPI = 0 to 5), medium (LPI = 5 to 15), high (LPI = 16 to 25) and very high (LPI = 26 to 56) risk zones in terms of application and sensitivity in the Rohingya refugee camp and surrounding area of Ukhiya, Cox's Bazar, Bangladesh. The prepared risk maps will provide a general understanding of the area's vulnerability to liquefaction and can be effectively used for seismic safety plans, design, and hazard mitigation programs. Moreover, it will help the camp inhabitants and local people in building their shelters (engineering structures) safely and economically. Based on the observed risks, it is recommended that Rohingya refugees must be temporarily relocated in a safer ground with the help of all concerned authorities. Bangladesh National Building Code (BNBC, 2020) [31] must be applied for future constructions & infrastructures development and design in the Ukhiya and surrounding areas to save lives and properties during high magnitude earthquakes.

There is currently no proper balance between the three (3) pillars (social, economic and environmental) of sustainable development in the camp area to manage hills as per the United Nations (UN) sustainable development goals (SDGs). The hidden earthquake risks might create big environmental as well as humanitarian disasters and crises in the investigated area. To mitigate these risks, sustainable geotechnical and geological engineering solutions such as ground improvement by applying different field compaction techniques, or facilitating water drainage by developing a drainage system are recommended. The grouting or deep mixing method before construction can also be recommended to stabilize the soft and loose soil of the Ukhiya Hills. Finally, the established risk maps will assist all concerned authorities, including planners, policymakers and engineers in developing guidelines to increase public awareness, promote sustainable infrastructure development, conduct seismic site characterization and mitigate the risks of liquefaction. Risk maps can also be used for future geological engineering works for sustainable planning, design and construction. This will ultimately save lives and protect properties during severe earthquake events and help to achieve sustainability in the Ukhiya-Teknaf regions of Cox's Bazar, Bangladesh.

Acknowledgements

The authors would like to acknowledge and appreciate "ANSO," China, for supporting this research and providing financial assistance.

Funding

Principal investigator (first author) of this research received funding from ANSO, China (Project No. ANSO-CR-PP-2020-08).

Data Availability Statement

Data are available on request.

Conflicts of Interest

The authors declare no conflicts of interest regarding the publication of this paper.

References

[1] Iwasaki, T., Tokida, K., Tatsuko, F. and Yasuda, S. (1978) A Practical Method for Assessing Soil Liquefaction Potential Based on Case Studies at Various Site in Japan. *Proceedings of the* 2*nd International Conference on Microzonation for Safer Construction Research and Application*, San Francisco, 26 November-1 December 1978, 885-896.

[2] Iwasaki, T., Tokida, K., Tatsuoka, F., Watanbe, S., Yasuda, S. and Sato, H. (1982) Microzonation for Soil Liquefaction Potential Using Simplified Methods. *Proceed-*

ings of the 3rd International Conference on Microzonation, Seattle, June 28-July 1, 1982.

[3] Chung, J.-W. and Rogers, J.D. (2011) Simplified Method for Spatial Evaluation of Liquefaction Potential in the St. Louis Area. *Journal of Geotechnical and Geoenvironmental Engineering*, **137**, 505-515. https://doi.org/10.1061/(ASCE)GT.1943-5606.0000450

[4] Cramer, C.H., Dhar, M.S. and Arellano, D. (2018) Update of the Urban Seismic and Liquefaction Hazard Maps for Memphis and Shelby County, Tennessee: Liquefaction Probability Curves and 2015 Hazard Maps. *Seismological Research Letters*, **89**, 688-701. https://doi.org/10.1785/0220170139

[5] Cramer, C.H., Rix, G.J. and Tucker, K. (2008) Probabilistic Liquefaction Hazard Maps for Memphis, Tennessee. *Seismological Research Letters*, **79**, 416-423. https://doi.org/10.1785/gssrl.79.3.416

[6] Haase, J.S., Choi, Y.S. and Nowack, R.L. (2011) Liquefaction Hazard near the Ohio River from Midwestern Scenario Earthquakes. *Environmental and Engineering Geoscience*, **17**, 165-181. https://doi.org/10.2113/gseegeosci.17.2.165

[7] Holzer, T.L., Bennett, M.J., Noce, T.E., Padovani, A.C. and Tinsley, J.C. (2006) Liquefaction Hazard Mapping with LPI in the Greater Oakland, California, Area. *Earthquake Spectra*, **22**, 693-708. https://doi.org/10.1193/1.2218591

[8] Juang, C.H. and Li, D.K. (2007) Assessment of Liquefaction Hazards in Charleston Quadrangle, South Carolina. *Engineering Geology*, **92**, 59-72. https://doi.org/10.1016/j.enggeo.2007.03.003

[9] Lenz, J.A. and Baise, L.G. (2007) Spatial Variability of Liquefaction Potential in Regional Mapping Using CPT and SPT Data. *Soil Dynamics and Earthquake Engineering*, **27**, 690-702. https://doi.org/10.1016/j.soildyn.2006.11.005

[10] Luna, R. and Frost, J.D. (1998) Spatial Liquefaction Analysis System. *Journal of Computing in Civil Engineering*, **12**, 48-56. https://doi.org/10.1061/(ASCE)0887-3801(1998)12:1(48)

[11] Maurer, B.W., Green, R.A., Cubrinovski, M. and Bradley, B.A. (2014) Evaluation of the Liquefaction Potential Index for Assessing Liquefaction Hazard in Christchurch, New Zealand. *Journal of Geotechnical and Geoenvironmental Engineering*, **140**, Article ID: 04014032. https://doi.org/10.1061/(ASCE)GT.1943-5606.0001117

[12] Toprak, S. and Holzer, T.L. (2003) Liquefaction Potential Index: Field Assessment. *Journal of Geotechnical and Geoenvironmental Engineering*, **129**, 315-322. https://doi.org/10.1061/(ASCE)1090-0241(2003)129:4(315)

[13] Hossain, Md Shakhawat, Kamal, A.S.M.M., Rahman, M.Z., Farazi, A.H., Mondal, D.R., Mahmud, T. and Ferdous, N. (2020) Assessment of Soil Liquefaction Potential: A Case Study for Moulvibazar Town, Sylhet, Bangladesh. *SN Applied Sciences*, **2**, Article No. 777. https://doi.org/10.1007/s42452-020-2582-x

[14] Kayal, J.R. (2010) Himalayan Tectonic Model and the Great Earthquakes: An Appraisal. *Geomatics*, *Natural Hazards and Risk*, **1**, 51-67. https://doi.org/10.1080/19475701003625752

[15] Wang, Y., Sieh, K., Tun, S.T., Lai, K.Y. and Myint, T. (2014) Active Tectonics and Earthquake Potential of the Myanmar Region. *Journal of Geophysical Research*: *Solid Earth*, **119**, 3767-3822. https://doi.org/10.1002/2013JB010762

[16] Bilham, R. and England, P. (2001) Plateau 'Pop-Up' in the Great 1897 Assam Earthquake. *Nature*, **410**, 806-809. https://doi.org/10.1038/35071057

[17] Dasgupta, S. and Mukhopadhyay, B. (2019) Revisiting Two Damaging Indian Earth-

quakes of 1885: Kashmir and Bengal. *Journal of the Geological Society of India*, **93**, 263-268. https://doi.org/10.1007/s12594-019-1172-2

[18] Hossain, M.S., Khan, M.S.H., Chowdhury, K.R. and Abdullah, R. (2019) Synthesis of the Tectonic and Structural Elements of the Bengal Basin and Its Surroundings. In: Mukherjee, S., Ed., *Tectonics and Structural Geology*: *Indian Context*. *Springer Geology*, Springer, Cham, 135-218. https://doi.org/10.1007/978-3-319-99341-6_6

[19] Kayal, J.R. (2014) Seismotectonics of the Great and Large Earthquakes in Himalaya. *Current Science*, **106**, 188-197.

[20] Islam, M.S., Huda, M.M., Al-Noman, M.N. and Al-hussaini. (2010) Attenuation of Earthquake Intensity in Bangladesh. 3*rd International Earthquake Symposium*, *Bangladesh* (*IBES*-3), Dhaka, 5-6 March 2010, 481-488.

[21] Stuart, M. (1920) The Srimangal Earthquake of 8th July, 1918. *Geological Magazine*, **46**, 1-70.

[22] Szeliga, W., Hough, S., Martin, S. and Bilham, R. (2010) Intensity, Magnitude, Location, and Attenuation in India for Felt Earthquakes since 1762. *Bulletin of the Seismological Society of America*, **100**, 570-584. https://doi.org/10.1785/0120080329

[23] Morino, M., Kamal, A.S.M.M., Akhter, S.H., Rahman, M.Z., Ali, R.M.E., Talukder, A., *et al*. (2014) A Paleo-Seismological Study of the Dauki Fault at Jaflong, Sylhet, Bangladesh: Historical Seismic Events and an Attempted Rupture Segmentation Model. *Journal of Asian Earth Sciences*, **91**, 218-226. https://doi.org/10.1016/j.jseaes.2014.06.002

[24] Morino, M., Maksud Kamal, A.S.M., Muslim, D., Ekram Ali, R.M., Kamal, M.A., Zillur Rahman, M. and Kaneko, F. (2011) Seismic Event of the Dauki Fault in 16th Century Confirmed by Trench Investigation at Gabrakhari Village, Haluaghat, Mymensingh, Bangladesh. *Journal of Asian Earth Sciences*, **42**, 492-498. https://doi.org/10.1016/j.jseaes.2011.05.002

[25] Morino, M., Monsur, M.H., Kamal, A.S.M.M., Akhter, S.H., Rahman, M.Z., Ali, R.M.E., Talukder, A. and Khan, M.M.H. (2014) Examples of Paleo-Liquefaction in Bangladesh. *The Journal of the Geological Society of Japan*, **120**, 7-8. https://doi.org/10.5575/geosoc.2014.0032

[26] Steckler, M.S., Mondal, D.R., Akhter, S.H., Seeber, L., Feng, L., Gale, J., Hill, E.M. and Howe, M. (2016) Locked and Loading Megathrust Linked to Active Subduction Beneath the Indo-Burman Ranges. *Nature Geoscience*, **6**, 615-618. https://doi.org/10.1038/ngeo2760

[27] Mondal, D.R., McHugh, C.M., Mortlock, R.A., Steckler, M.S., Mustaque, S. and Akhter, S.H. (2018) Microatolls Document the 1762 and Prior Earthquakes along the Southeast Coast of Bangladesh. *Tectonophysics*, **745**, 196-213. https://doi.org/10.1016/j.tecto.2018.07.020

[28] Bürgi, P., Hubbard, J., Akhter, S.H. and Peterson, D.E. (2021) Geometry of the Décollement below Eastern Bangladesh and Implications for Seismic Hazard. *Journal of Geophysical Research*: *Solid Earth*, **126**, e2020JB021519. https://doi.org/10.1029/2020JB021519

[29] Hossain, M.S., Xiao, W., Khan, M.S.H., Chowdhury, K.R. and Ao, S. (2020) Geodynamic Model and Tectono-Structural Framework of the Bengal Basin and Its Surroundings. *Journal of Maps*, **16**, 445-458. https://doi.org/10.1080/17445647.2020.1770136

[30] Sakawat Hossain, M., Masumur Rahaman, M. and Khan, R.A. (2020) Active Seismic Structures, Energy Infrastructures, and Earthquake Disaster Response Strategy—Bangladesh Perspective. *International Energy Journal*, **20**, 509-522.

[31] BNBC (2021) Bangladesh National Building Code (BNNC) 2020.2, 1999-2001.

[32] Hossain, A.T.M.S., Dutta, T., Mahabub, M.S., Haque, M.E., Khatun, M., Sayem, M.H., Imam, H., Jafrin, S.J., Khan, P. and Bakali, R., (2022) Liquefaction Potentiality Index Based Risks in the Rohingya Refugee Camps of Ukhiya, Cox's Bazar, Bangladesh—A Threat For Sustainable Community Living. *GSA Connects* 2022 *Meeting in Denver*, Colorado, USA, 9-12 October 2022. https://doi.org/10.1130/abs/2022AM-378674

[33] Kamal, A.S.M.M., Hossain, F., Rahman, M.Z., Ahmed, B. and Sammonds, P. (2022) Geological and Soil Engineering Properties of Shallow Landslides Occurring in the Kutupalong Rohingya Camp in Cox's Bazar, Bangladesh. *Landslides*, **19**, 465-478. https://doi.org/10.1007/s10346-021-01810-6

[34] Alam, M.K., Hasan, A.K.M.S., Khan, M.R. and Whitney, J.W. (1990) Geological Map of Bangladesh. Geological Survey of Bangladesh, Dhaka.

[35] Mahabub, M.S., Hossain, A.T.M.S. and Pahlowan, E.U.D. (2020) Assessment of Liquefaction Potential from Sirajganj to Kurigram Area, Bangladesh. *IOSR Journal of Mechanical and Civil Engineering*, **17**, 31-43.

[36] Dutta, T., (2022) Earthquake Induced Liquefaction Risk Assessment in the Rohingya Refugee Camps of Ukhiya. Cox's Bazar, Bangladesh.

[37] Imam, H., Hossain, A.T.M.S., Sayem, H., Haque, E., Jafrin, S.J., Khan, P.A. and Bakali, R. (2023) Shallow Landslide Site Characterization using Electrical Resistivity Technique (ERT) at Balukhali Rohingya Refugee Camps of Ukhiya, Cox's Bazar, Bangladesh. *European Journal of Engineering and Technology Research*, **8**, 46-53. https://doi.org/10.24018/ejeng.2023.8.1.2932

[38] BS 5930 (1999) Code of Practice for Site Investigations. British Standard.

[39] LiquefyPro CivilTech Software (2015) Civil Tech.

[40] BS1377 (1990) British Standard Methods of Test for Soils for Civil Engineering Purposes. British Standards.

[41] American Society for Testing and Materials (1992) Annual Book of ASTM Standards. American Society for Testing and Materials, Philadelphia.

[42] Seed, H.B. and Idriss, I.M. (1971) Simplified Procedure for Evaluating Soil Liquefaction Potential. *Journal of the Soil Mechanics and Foundations Division*, **97**, 1249-1273. https://doi.org/10.1061/JSFEAQ.0001662

[43] Harder, L.F.J. and Boulanger, R.W. (1997) NCEER Workshop on Evaluation of Liquefaction Resistance of Soils.

[44] Seed, H.B. and Idriss, I.M. (1982) Ground Motion and Soil Liquefaction during Earthquakes. In *Monograph Series*, Earthquake Engineering Research Institute Monograph, Oakland.

[45] Seed, H.B. (1979) Soil Liquefaction and Cyclic Mobility Evaluation for Level Ground during Earthquakes. *Journal of the Geotechnical Engineering Division*, **105**, 201-255. https://doi.org/10.1016/0148-9062(79)91243-9

[46] Seed, H.B., Idriss, I.M. and Arango, I. (1983) Evaluation of Liquefaction Potential Using Field Performance Data. *Journal of Geotechnical Engineering*, **109**, 458-482. https://doi.org/10.1061/(ASCE)0733-9410(1983)109:3(458)

[47] Seed, H.B., Tokimatsu, K., Harder, L.F. and Chung, R.M. (1985) Influence of SPT Procedures in Soil Liquefaction Resistance Evaluations. *Journal of Geotechnical Engineering*, **111**, 1425-1445. https://doi.org/10.1061/(ASCE)0733-9410(1985)111:12(1425)

[48] Tokimatsu, K. and Seed, H.B. (1987) Evaluation of Settlements in Sands due to Earth-

quake Shaking. *Journal of Geotechnical Engineering*, **113**, 861-878.
https://doi.org/10.1061/(ASCE)0733-9410(1987)113:8(861)

[49] Youd, T.L. and Idriss, I.M. (1997) Proceeding of the NCEER Workshop on Evaluation of Liquefaction Resistance of Soils. Technical Report NCEER-97-0022. National Center for Earthquake Engineering Research, New York.

[50] Youd, T.L., Idriss, I.M. andrus, R.D., Arango, I., Castro, G., Christian, J.T., *et al.* (2001) Liquefaction Resistance of Soils: Summary Report from the 1996 NCEER and 1998 NCEER/NSF Workshops on Evaluation of Liquefaction Resistance of Soils. *Journal of Geotechnical and Geoenvironmental Engineering*, **127**, 817-833.
https://doi.org/10.1061/(ASCE)1090-0241(2001)127:10(817)

[51] Robertson, P.K. and Wride, C.E. (1998) Evaluating Cyclic Liquefaction Potential Using the Cone Penetration Test. *Canadian Geotechnical Journal*, **35**, 442-459.
https://doi.org/10.1139/t98-017

[52] LiquefyPro, Version 5 (2011) Liquefaction and Settlement Analysis Software Manual. CivilTech Software.

[53] (2011) ASTM D 2487: Standard Practice for Classification of Soils for Engineering Purposes (Unified Soil Classification System). ASTM International, West Conshohocken.

[54] Tsuchida, H. (1970) Prediction and Countermeasure against Liquefaction in Sand Deposits. In: *The Seminar of the Port and Harbour Research Institute*, 1-33.

[55] Iwasaki, T. (1986) Soil Liquefaction Studies in Japan: State-of-the-Art. *Soil Dynamics and Earthquake Engineering*, **5**, 2-68.
https://doi.org/10.1016/0267-7261(86)90024-2

[56] Bowles, J.E. (1979) Physical and Geotechnical Properties of Soils. McGraw-Hill, New York.

[57] Grim, R.E. (1962) Applied Clay Mineralogy. *Geologiska Föreningen i Stockholm Förhandlingar*, **84**, 533. https://doi.org/10.1080/11035896209447314

[58] Bowles, J.E. (1997) Foundation Analysis and Design. McGraw-Hill, New York.

[59] UN Sustainable Development Goals. https://sdgs.un.org/goals

[60] United Nations (2015) Transforming Our World: The 2030 Agenda for Sustainable Development. United Nations Sustainable Knowledge Platform. Sustainable Development Goals.